UNIVERSITAT DE BARCELONA

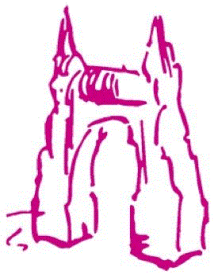

UNIVERSITAT DE BARCELONA

FACULTY OF PHARMACY AND FOOD SCIENCE

BACHELOR'S THESIS

June 2018

STERYL ESTER BIOSYNTHESIS IN PLANTS

Marta Riba Baqués

Main field: Biochemistry and Molecular Biology

Secondary fields: Plant Physiology and Microbiology

ACKNOWLEDGMENTS

I would like to offer my special thanks to my main supervisor for giving me the opportunity to work in a leading-edge centre and collaborate with an excellent research group. I would also like to express my very great appreciation to him for his willingness, guidance, encouragement and useful critiques of this research work.

I wish to acknowledge the help provided by all members of the research group "Isoprenoid metabolism in tomato: Involvement in development and stress responses" of the Centre for Research in Agricultural Genomics (CRAG), especially PhD student Alma Burciaga Monge for her advice and constructive recommendations, and my workmate Joan Manel López Tubau for valuable support.

INDEX

ABSTRACT

Sterol biosynthesis in plants

Plant sterols are found in free form (free sterols, FS) and conjugated as steryl esters (SEs), steryl glucosides (SGs) and acylated steryl glucosides (ASGs). Conjugated sterols are ubiquitously found in plants, however their relative contents may differ among species. Specially, in genus *Solanum* plants, such as tomato, glycosylated sterols are found in a high amount, whereas in most plant species they are minor components. The SEs play a central role in the maintenance of homeostasis of membrane FS. The synthesis of SEs is catalyzed by sterol acyltransferases. Depending on the acyl donor substrate, sterol acyltransferases can be categorized into two main groups: acyl-CoA:sterol acyltransferases (ASAT) and phospholipid:sterol acyltransferases (PSAT). So far only ASAT and PSAT from *Arabidopsis thaliana* and tomato (*S. lycopersicum*) have been cloned and characterized. SlASAT localizes in the plasma membrane while AtASAT localizes in the endoplasmic reticulum. SlASAT and AtASAT share significant sequence identity but differ in length due to a central domain of 101 amino acids in SlASAT which has only 18 amino acids in the equivalent region of AtASAT. In this work, a strategy of overlapping extension PCR has been designed and implemented to obtain a chimeric cDNA encoding a hybrid ASAT in which the central domain of SlASAT has been replaced by the equivalent domain of AtASAT, as a first step to investigate the biological role of this ASAT protein domain. Moreover, a restriction fragment length polymorphism (RFLP) strategy has been devised and successfully applied to identify tomato homozygous knock-out mutants generated by CRISPR-Cas9.

RESUM

Biosíntesi dels esterols en les plantes

Els esterols vegetals es troben en forma lliure (FS) i conjugada, com a esteril èsters (SEs), esteril glucòsids (SGs) i acil esteril glucòsids (ASGs). Els esterols conjugats són components àmpliament distribuïts en les plantes, però el seu contingut relatiu difereix entre les diferents espècies. En el gènere *Solanum*, com la tomaquera, els esterols glicosilats es troben en una proporció elevada, mentre que en la major part de les plantes són minoritaris. Els SEs tenen un paper rellevant en el manteniment de l'homeòstasi dels FS de membrana. La síntesi dels SEs està catalitzada per les esterol acil transferases. Depenent del substrat, aquestes es classifiquen en: acil-CoA:esterol acil transferases (ASAT) i les fosfolípid:esterol acil transferases (PSAT). Actualment, només les ASAT i PSAT d'*Arabidopsis thaliana* i tomaquera (*S. lycopersicum*) han estat clonades i caracteritzades. SlASAT es localitza a la membrana plasmàtica, en canvi, AtASAT es troba al reticle endoplasmàtic. Les seqüències d'SlASAT i AtASAT comparteixen una homologia significativa, però difereixen en longitud a causa del domini central de 101 aminoàcids d'SlASAT, el qual consta només de 18 aminoàcids en la regió equivalent d'AtASAT. En aquest treball, s'ha dissenyat i aplicat una estratègia d'extensió per PCR solapant per obtenir una seqüència de cDNA quimèrica que codifica per una proteïna ASAT híbrida, en la qual el domini central d'SlASAT ha estat reemplaçat pel domini equivalent d'AtASAT, com a un primer pas per a l'estudi d'aquest domini proteic. A més, s'ha ideat i aplicat una estratègia de polimorfisme de longitud dels fragments de restricció (RFLP) per identificar mutants *knock-out* de tomàquet de tipus homozigot generats mitjançant la tècnica CRISPR-Cas9.

INTEGRATION OF THE DIFFERENT FIELDS

This bachelor thesis is a report of an experimental work carried out as part of a broader project aimed at studying the biological role of enzymes PSAT and ASAT involved in plant sterol ester synthesis. This assays cover different fields addressed throughout the Pharmacy Degree.

One of these areas is Plant Physiology, since the work has to do with the study of plant metabolism and, in particular, the synthesis of steryl esters and the biological role of these metabolites in plants.

Another area covered by this work is Microbiology due to the use of methods such as bacterial transformation, which involves, among other things, preparing solid and liquid media for bacterial cell growth, manipulating microbial strains and, ultimately, applying the theoretical knowledge acquired in relation to their structure, physiology and genetics.

The main field of this study is Biochemistry and Molecular Biology. Theoretical and practical knowledge about proteins, enzymes, enzymatic catalysis and metabolism acquired throughout the Degree has been essential for the development of the thesis. In addition, the knowledge acquired during the Degree on the structure and function of nucleic acids, how the genetic information flows from DNA to proteins, and a series of recombinant DNA and genetic engineering techniques has also been crucial to achieve the objectives proposed initially.

1. INTRODUCTION

Sterols are essential components of most eukaryotic cell membranes that play a key role in determining membrane structure and function (Schaller, 2004). Actually, they regulate membrane fluidity, permeability and elasticity, and have been shown to modulate the activity of membrane-bound proteins (Hartmann, 1998). Sterols are also precursors for the biosynthesis of hormones, including brassinosteroids, a class of plant hormones known to play a key role in different biological processes, as plant development, morphogenesis and growth (Wang & al., 2012). Moreover, sterols are implicated in plant responses to biotic and abiotic stresses (Ramirez-Estrada & al., 2017).

The structure of sterols is formed by the cyclopentane-perhydrophentanthrene ring system consisting of four rigid rings with a free hydroxyl group at C3 position (Fig. 1). Plant sterols, also called phytosterols, differ from animal sterols, where cholesterol is most often the only end product of sterol biosynthesis, in the nature of the side chain at position C17 and the number and position of methyl groups and double bonds in the molecule (Ostlund, 2002).

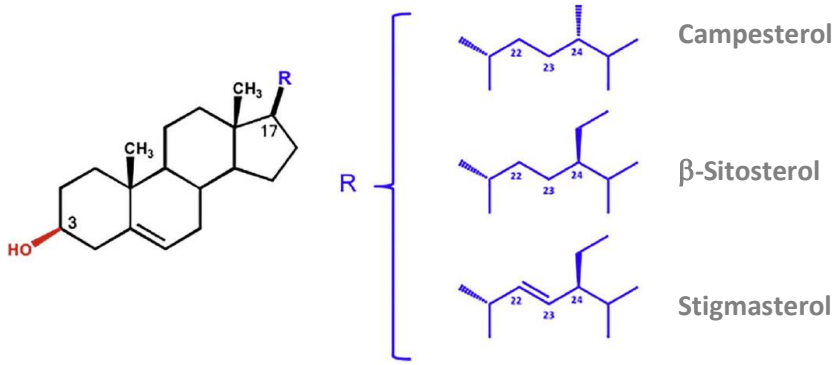

Fig. 1. Most common sterols in plants (Ferrer & al., 2017).

Plant sterols are formed from the C5 precursor isopentenyl diphosphate (IPP) synthetized through the mevalonic acid (MVA) pathway. IPP is then converted to its isomer dimethylallyl diphosphate (DMAPP), which condensates sequentially with two molecules of IPP yielding the C15 intermediate farnesyl diphosphate (FPP). Subsequently, two units of FPP condensate to produce the linear C30 compound squalene, which is the first committed precursor of sterol and triterpenoid biosynthesis (Fig. 2) (Vranová & al., 2012).

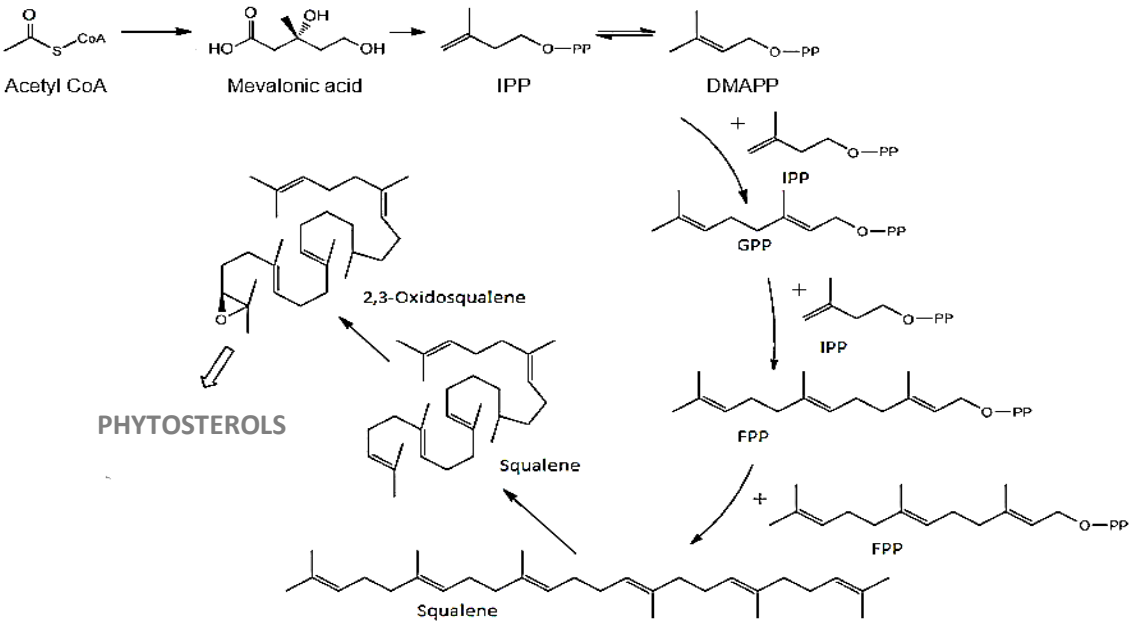

Fig. 2. Biosynthesis of squalene, the first committed precursor of the sterol pathway, from acetil-CoA. IPP, isopentenyl diphosphate; DMAPP, dimethylallyl diphosphate; GPP, geranyl diphosphate; FPP, farnesyl diphosphate (Netala & al., 2015).

In higher plants, the three most common sterols are β-sitosterol, stigmasterol and campesterol (Fig. 1). Phytosterols are found in free form (free sterols, FS) and conjugated as steryl glucosides (SGs), acylated steryl glucosides (ASGs) and fatty acyl sterol esters or steryl esters (SEs) (Fig. 3) (Moreau & al., 2002).

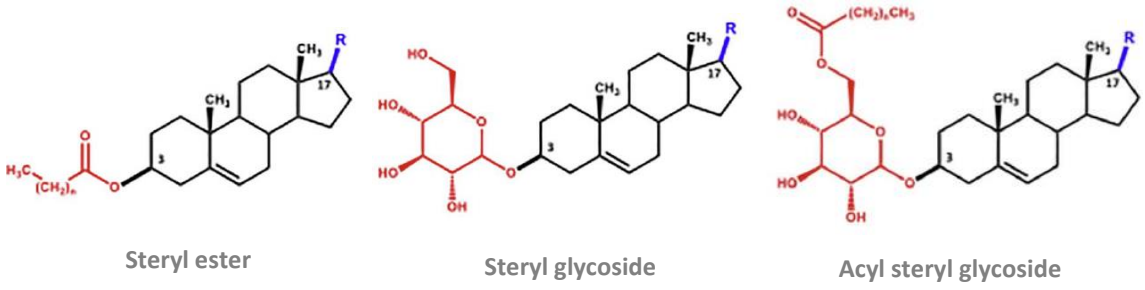

Fig. 3. Structure of conjugated sterols. SEs have a hydroxyl group at C3 position esterified with a fatty acid. In SGs, the C3 hydroxyl group of the sterol moiety have a sugar linked through a β-glycosidic bond. ASGs are derivatives of SGs in which the hydroxyl group of the C6 position of the sugar moiety is esterified with a fatty acid (Ferrer & al., 2017).

SGs, ASGs and SEs derive from FS, through enzymatic reactions. Specifically, sterol acyltransferases catalyse the formation SEs whereas sterol glycosyltransferases synthesize steryl glycosides, which may be subsequently converted into acyl steryl glycosides by steryl glycoside acyltransferases (Fig. 4) (Ferrer & al., 2017).

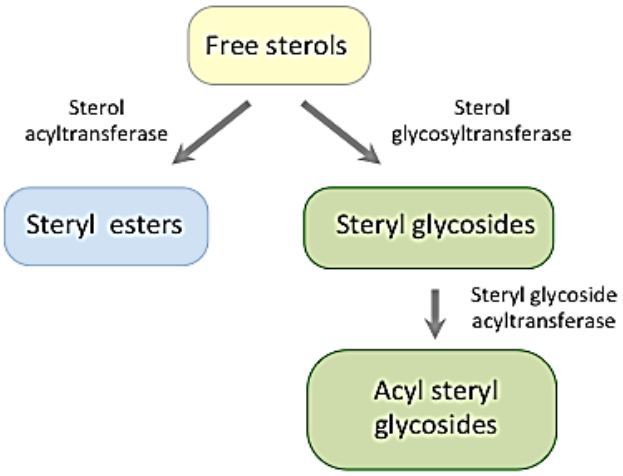

Fig. 4. Representation of the biosynthesis of conjugated sterols showing the enzymatic activities involved (Ferrer & al., 2017).

Conjugated sterols are found in a widespread way in higher plants. However, their total levels and their relative contents may greatly differ among species and among organs and tissues within a single organism. Besides, their profile may change in response to developmental and environmental factors. It is noteworthy to mention the high content of SGs and ASGs in genus *Solanum* plants, such as tomato plant, in contrast to most plant species in which these conjugated forms of sterols are minor components (Duperon & al., 1984; Nyström & al., 2012). In the evolutionary process, this feature is suggested to improve on the protection of cell membrane integrity in those species that also accumulate high levels of steroidal glycoalkaloids (Murphy, 2012).

While FS**,** SGs and ASGs are located in cell membranes, SEs localize in cytoplasmic lipid vesicles, also called lipid droplets, (Bouvier-Nave & al., 2010) which serve as a storage pool of sterols involved in the maintenance of membrane FS homeostasis. Moreover, SEs can be mobilized from lipid droplets to sustain the cell needs of FS in actively growing tissues. For example, the accumulation of SEs observed during seed maturation (Dyas & Goad, 1993; Harker & al., 2003) would be necessary to supply the FS required for seedling growth during the early stages of plant growth, whereas the enrichment of SEs in senescing tissues seems to participate in the recycling of FS and the fatty acids released from disorganized cell membranes in aging tissues (Duperon & al., 1984; Bouvier-Nave & al., 2010). An important increase of SEs levels has also been reported to occur during tomato fruit ripening, although the biological significance of this change is so far unknown (Whitaker, 1988).

The synthesis of SEs is catalyzed by a group of enzymes collectively known as sterol acyltransferases. Depending on whether the acyl donor substrate is a long-chain fatty acyl-CoA or a phospolipid, sterol acyltransferases can be categorized into two main groups, namely acyl-CoA:sterol acyltransferases (ASAT) (EC 2.3.1.26) and phospholipid:sterol acyltransferases (PSAT) (EC 2.3.1.43), respectively. So far only ASAT and PSAT enzymes from *Arabidopsis thaliana* and tomato (*Solanum lycopersicum* cv Micro-Tom) have been cloned and functionally characterized (Banaś & al., 2005; Chen & al., 2007; Lara & al., 2018).

SlASAT and AtASAT share significant sequence homology (Fig. 6). Nevertheless, they are substantially different in length: SlASAT consists of 444 amino acids whereas AtASAT contains 345 amino acids. This different length is mainly due to a stretch of 101 amino acids comprised between positions 118 and 218, both included, in the SlASAT sequence, which in the AtASAT equivalent region consists of only 18 amino acids comprised between positions 104 to 121, both included. Additionally, SlASAT is located in the plasma membrane while AtASAT localizes in the endoplasmic reticulum (ER) (Lara & al., 2018). The predicted membrane topology models of SlASAT and AtASAT performed with the Protter 1.0 program (Omasits & al., 2014) are shown in Figure 5.

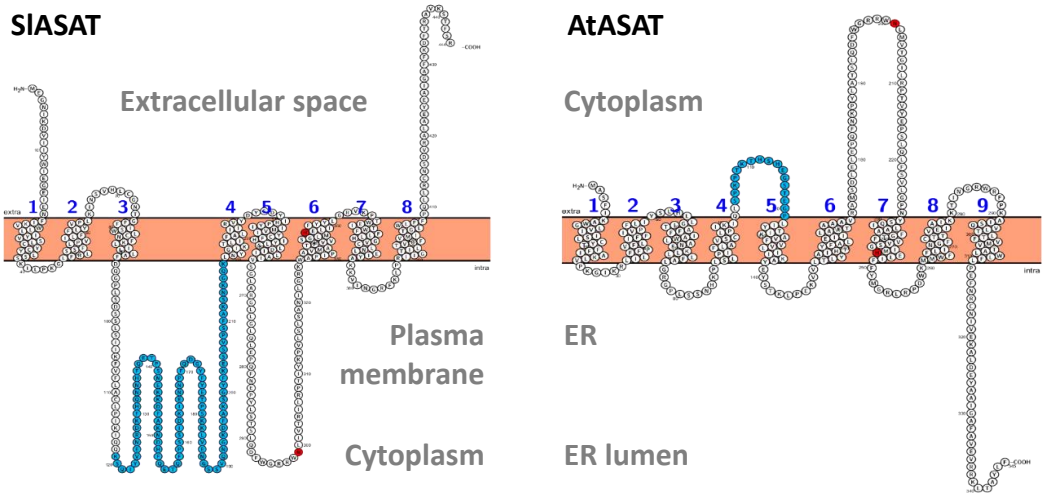

Fig. 5. Membrane topology models of SlASAT1 and AtASAT1. The transmembrane sequences are numbered in blue. The Asn and His residues reportedly important for ASAT catalysis are shown in red. The sequence of 101 amino acid residues comprised between positions 118 to 218 in the SlASAT1 sequence, and the equivalent sequence of 18 amino acids comprised between positions 104 to 121 in the AtASAT1 sequence are shown in blue.

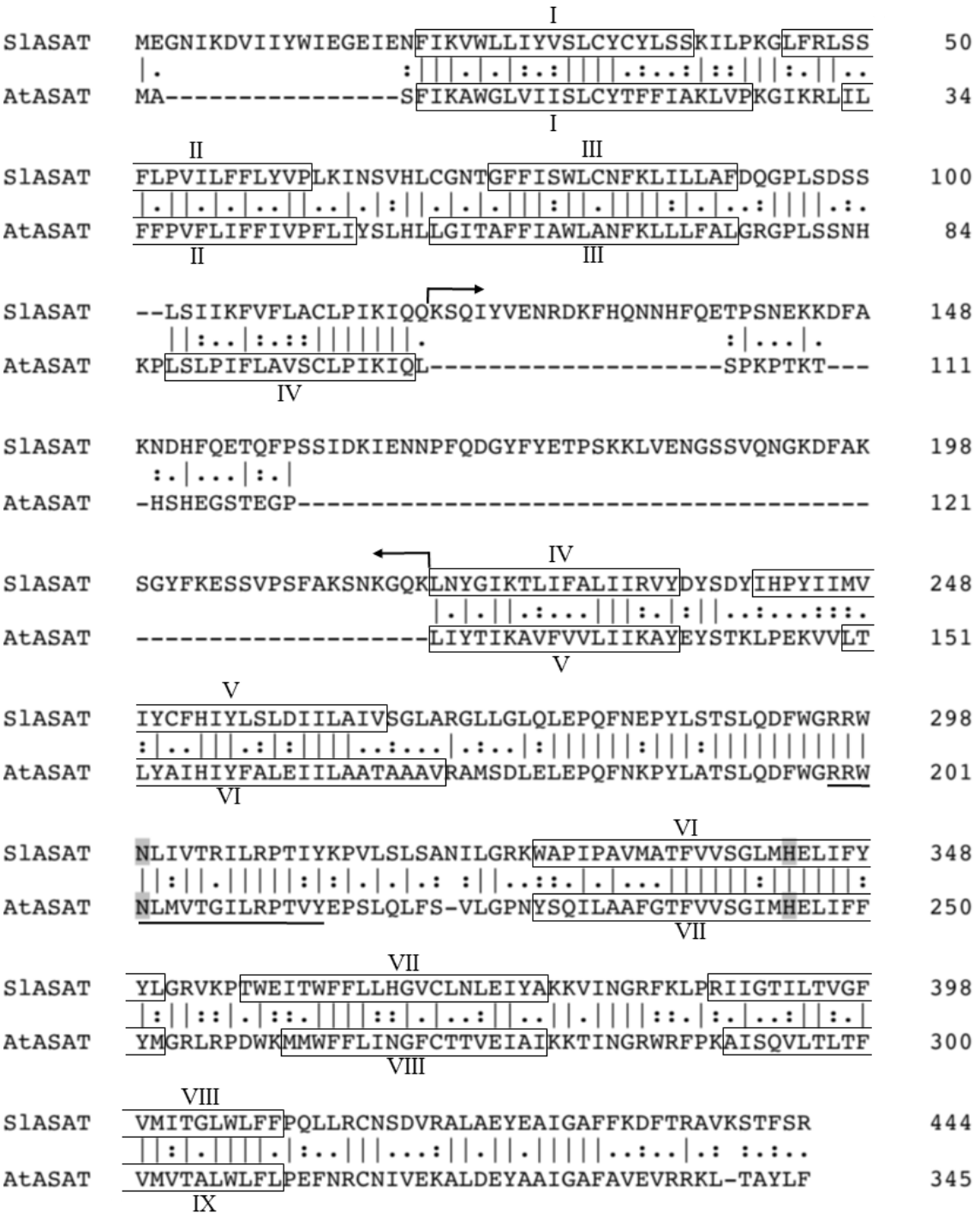

Fig. 6. AtASAT and SlASAT alignment by Clustal Omega software (European Bioinformatics Institute, 2016). The amino acid numbering is shown at the right side. Vertical bars symbolise conserved amino acid residues in both sequences. Two dots mean high similarity of amino acid residues and one dot low similarity of amino acid residues, among both sequences. Hyphens found through protein sequences are spaces generated to optimize the alignment. Predicted hydrophobic transmembrane domains are boxed (I-VII SlASAT and I-IX AtASAT). Catalytic residues Asn and His, found in a conserved hydrophilic domain, are shown on grey background.

Tomato is one of the most important horticultural crops worldwide, and a well-established model plant for research in fleshy fruit development and ripening (Giovannoni, 2004), two biological processes in which SEs appears to play an important role. Some recent evidence also suggests that SEs might be involved in mediating plant defence responses against pathogen attack (Kopischke & al., 2013). All these observations prompted the research group "Isoprenoid metabolism in tomato: Involvement in development and stress responses" at the Centre for Research in Agricultural Genomics (CRAG) to undertake a research project aimed at the characterization of the PSAT and ASAT enzymes of the dwarf tomato variety *Solanum lycopersicum* cv. Micro-Tom, as a first step toward the elucidation of the biological role of SEs biosynthesis in tomato growth and development as well as in the adaptation to stress conditions.

This bachelor thesis is focused on studying sterol acyltransferases involved in the synthesis of tomato SEs. On the one hand, the research group is currently generating tomato *psat* knock-out mutants by CRISPR-Cas9 technology, in order to investigate the role of this enzyme in tomato plant and fruit growth and development as well in the adaptive response to stress conditions. In this context, the availability of quick and effective methods to distinguish mutant plants from wild-type individuals would greatly facilitate the mutant selection process.

On the other hand, the research group is interested in investigating the role of the 101 amino acids insertion found in SlASAT. In this work, a strategy of extension for overlapping polymerase chain reaction (OE-PCR) (Lee & al., 2004) has been designed and implemented successfully to obtain a hybrid cDNA sequence encoding a chimeric ASAT protein in which the 101 amino acid region of SlASAT has been replaced by the 18 amino acids of the equivalent region of AtASAT (Fig. 6). Due to the relative position of protein domains in the designed chimeric protein SlASAT-AtASAT-SlASAT (tomato-Arabidopsis-tomato), it was called *TAT* ASAT. The availability of this chimeric protein will allow future subcellular location studies to be addressed in order to determine whether this protein domain is involved or not in the differential subcellular location of these two enzymes or if it may have an influence on enzyme activity.

2. OBJECTIVES

The main objectives of the thesis are:

- To design a rapid and efficient method to discriminate *psat* homozygous and heterozygous knock-out tomato mutants from wild-type individuals.
- To obtain a chimeric acyl-CoA:sterol acyltransferase (ASAT) protein from Arabidopsis and tomato ASAT proteins.

3. MATERIALS AND METHODS

3.1. MATERIALS

Thermostable DNA polymerases used for PCR (Polymerase Chain Reaction) amplification:

- Invitrogen™ Pfx50™ DNA Polymerase (Thermo Fisher Scientific®): high-fidelity polymerase based on recombinant DNA polymerase from *Thermococcus zilligii*, with proofreading (3'→5' exonuclease) activity, fused to an accessory protein which stabilizes primer-template complexes. In fact, the fusion enzyme has 50 times higher fidelity than *Taq* DNA polymerase.
- Green *Taq* DNA Polymerase (GenScript®): thermostable polymerase without proofreading activity. The enzyme has a high thermal stability and PCR yield.

Fragment	Primer sequence		Tm (°C)
AB	Fw (a)	5'-GGGGACAAGTTTGTACAAAAAAGCAGGCTTCATGGAGGG AAATATTAAAGATG-3'	65.9
	Rv (b)	5'-TGGGCTCAGTTGAATCTTGATAGGTAAACA-3'	59.4
CD	Fw (c)	5'-CAAGATTCAACTGAGCCCAAAACCTAC-3'	58.0
	Rv (d)	5'-GCCATAATTTAAAGGACCCTCTGTGGATCC-3'	60.4
EF	Fw (e)	5'-GAGGGTCCTTTAAATTATGGCATAAAG-3'	54.2
	Rv (f)	5´-GGGGACCACTTTGTACAAGAAAGCTGGGTCTCTCGAAAAT GTTGATTTCACAGC-3´	68.4

Table 1. Primers employed to obtain the three ASAT fragments AB (5'-region of SlASAT), CD (central part of AtASAT) and EF (3'-region of SlASAT) used to generate the chimeric *TAT* ASAT cDNA by overlapping PCR. The sequences corresponding to the SlASAT cDNA sequence are shown in red whereas those corresponding to AtASAT are shown in green. Outermost primers A and F include *att*B sequences (black) at their 5' end that were needed for homologous recombination-based cloning of the final chimeric cDNA fragment into the appropriate vector. The *att* sequences have not been considered to estimate primer Tm (OligoAnalyzer 3.1 Tool).

Primers employed to ensure the recombination process at final vector pEarley Gate 103:

- Primer e (Table 1)
- Primer GFP Rv: 5'-GTAGTGACAAGTGTTGGCCACGG-3' (Tm 60.3 °C, estimated by OligoAnalyzer 3.1 Tool).

Enzymes employed for homologous recombination-based cloning:

- Gateway™ BP Clonase™ II enzyme mix (Thermo Fisher Scientific®): enzyme and buffer formulation involving the bacteriophage lambda recombination protein Integrase (Int), the *E. coli*-encoded protein Integration Host Factor (IHF), and reaction buffer contained in a single mix. The enzyme mix catalyzes *in vitro* recombination between an *att*B PCR product, or an *att*B- containing expression clone, and an *att*P-containing donor vector to obtain an *att*L-containing entry clone. The kit includes Proteinase K Solution (2 μg/μl), a serine protease that stops recombination reaction.
- Gateway™ LR Clonase™ II enzyme mix (Thermo Fisher Scientific®): enzyme and buffer formulation involving the bacteriophage lambda recombination proteins Integrase (Int) and Excisionase (Xis), the *E. coli*-encoded protein Integration Host Factor (IHF), and reaction buffer contained in a single mix. The enzyme mix catalyzes *in vitro* recombination between an entry clone containing and *att*L-flanked sequence and an *att*R-containing destination vector to obtain an *att*B-containing expression clone. The kit includes Proteinase K Solution (2 μg/μl).

Restriction enzyme utilized to detect tomato PSAT CRISPR-Cas9 knock-out mutants:

- *Xho*I (Promega®): enzyme obtained from *Xanthomonas holcicola* which recognises C^TCGAG sites. The optimum reaction temperature is 37°C.

Materials employed to run DNA electrophoresis:

- Agarose (Conda®): polysaccharide based on α-galactose and β-galactose extracted from *Gellidium* and *Gracillaria*.
- DNA ladders (Thermo Fisher Scientific®): mix of DNA fragments designed for sizing and approximate quantification of double-stranded DNA on agarose gel.

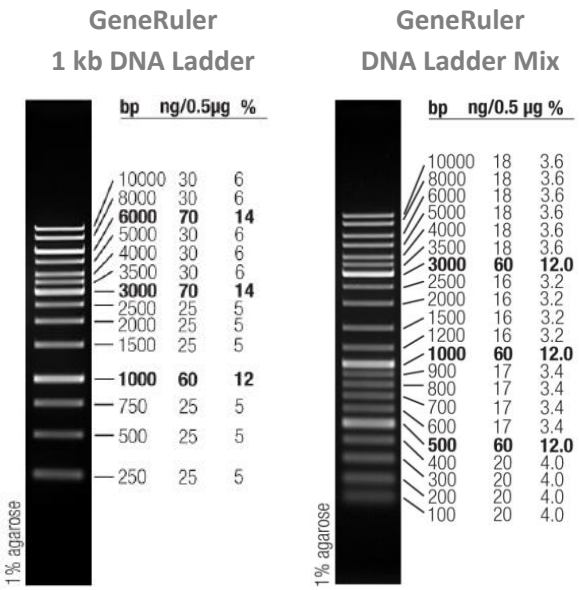

Fig. 7. DNA ladders employed.

- SYBR® Safe (Thermo Fisher Scientific®): cyanine dye used as nucleic acid stain. It binds DNA resulting in a DNA-dye-complex for visualization of DNA in agarose gels. This stain is a safer alternative to the mutagen ethidium bromide.
- 6X DNA Loading Dye (Thermo Fisher Scientific®): loading dye contains bromophenol blue and xylene cyanol FF. It is used for loading DNA markers and samples on agarose gels and allows an easy visual tracking of DNA migration during electrophoresis.

Kits to purify plasmids and DNA fragments:

- Wizard® Plus SV Minipreps DNA Purification System (Promega®) for rapid isolation of plasmid DNA from *E. coli* cell cultures.
- Wizard® SV Gel and PCR Clean-Up System (Promega®): membrane-based system for purification of DNA fragments of 100 bp to 10 kb from agarose gels and PCR products directly from an amplification reaction to remove excess nucleotides and primers.

Growth media for *E. coli* strains:

- Luria-Bertani (LB), pH 7.0:

  Tryptone……10.0 g/L

  Yeast Extract……5.0 g/L

  Sodium Chloride……5.0 g/L

When required, LB medium was supplemented with kanamycin or gentamycin at a final concentration of 25 µg/mL each so as to select transformed colonies carrying an antibiotic resistance gene provided by a plasmid.

Bacterial strain:

- TOP10 Chemically competent *E. coli* cells (Thermo Fisher Scientific®)
  F– *mcr*A Δ(*mrr-hsd*RMS-*mcr*BC) Φ80*lac*ZΔM15 Δ*lac*X74 *rec*A1 *ara*D139 Δ(*ara leu*) 7697 *gal*U *gal*K *rps*L (StrR) *end*A1 *nup*G 15.

Gateway® vector for recombination-based cloning (Thermo Fisher Scientific®):

- pDONR™ 207: Gateway® donor vector with *att*P1 and *att*P2 sites and a gentamycin resistance marker.
- pEarley Gate 103: Gateway® vector which contains *att*P1 and *att*P2 sites and a kanamycin resistance marker gene. It allows recombination-based cloning of cDNAs from Gateway® entry vectors to express C-terminal protein fusions with GFP and 6xHis in plants under control of the strong constitutive promoter CaMV (Cauliflower Mosaic Virus) 35S promoter.

Fig. 8. Scheme of pDONR™ 207 and pEarleyGate 103 vectors designed by SnapGene® software (GSL Biotech, 2018).

3.2. METHODS

3.2.1. Preparation of solid and liquid media

Sterile solid LB growth medium is stored in glass flasks. Immediately before use, the flask is placed into the microwave oven for 12 minutes at 300W to melt LB media. Liquefied medium is then cooled at 45-50 °C. Stocks of antibiotics at the appropriate concentrations are also previously prepared and available in the laboratory (Table 2). The appropriate volume of antibiotic stock solution is added to the liquid LB medium to reach the final concentration required. LB medium is then poured into empty, sterile Petri dishes in a laminar flow cabinet and left there until the medium solidifies. Finally, Petri dishes are stored wrapped at 4 °C.

Antibiotic	Stock concentration (mg/mL)	Working concentration (µg/mL)
Gentamicin	100	25
Kanamycin	25	25

Table 2. Stock concentration and working concentration of antibiotics added to LB growth medium.

LB liquid medium is prepared as described above but without agar. Antibiotics are added at the same final concentrations shown in Table 2.

3.2.2. Preparation of agarose gel electrophoresis 1%

In order to prepare agarose gels at 1%, weight 0.1 g of agarose for every 10 mL of Tris-Boric acid-EDTA (TBE) 1X Buffer. The volume of the gel depends on the size of the casting tray. For the smallest gel trays, 30-40 mL is a convenient volume, and for the biggest one, 100-120 mL. After mixing TBE and agarose in a flask, it is brought to a boil in a microwave oven to achieve the complete dissolution of agarose. After letting it a bit cooler, 1 µL of SYBR® Safe is added for every 12 mL of solution. It is mixed and poured into the gel casting tray. The wells of the gel are made by inserting a comb into the slots in the casting tray. Agarose solidifies around the comb and wells are formed.

Even though SYBR® Safe is a safer alternative to ethidium bromide, it is also a DNA intercalating agent. Thus, it has to be handled with care, paying attention on security rules and using always gloves to avoid contamination.

3.2.3. PCR reaction using Green *Taq* Polymerase

A standard PCR mixture consisted of:

Component	Volume (µL)
Green *Taq* Mix (5 U/µL)	5
Primer Fw (10 µM)	1
Primer Rv (10 µM)	1
DNA template (10 ng/µL)	1
Autoclaved milliQ water	2
Final Volume	10

Table 3. Standard PCR mix using Green *Taq* Polymerase. Green *Taq* Mix contain dNTPs.

Step	Temperature (°C)	Time	
1	94	5 min	Initial template denaturation
2	94	30 s	Template denaturation
3	50.7-67.4 / 50 / 54*	1 min	Annealing
4	72	1 min	Extension 1 min/kb DNA template
5	72	8 min	Final extension

Table 4. Thermocycling conditions for a PCR routine with Green *Taq* Polymerase. Steps 2 to 4 are repeated 30 times. *Selected annealing temperatures were: 50.7-67.4 °C in gradient PCR (section 4.2.1), 50 °C in PCR after BP reaction and 54 °C in PCR after LR reaction (section 4.2.4), according to Tm of primer pair used.

3.2.4. PCR reaction using Invitrogen™ Pfx50™ DNA Polymerase

Component	Volume (µL)
10X Pfx50™ PCR Mix	5
10 µM dNTP Mix	1.5
Primers (10 µM, each one)	1.5 each one (final concentration of 0.3 µM per primer)
DNA template	≥1 (10 ng)
Pfx50™ DNA Polymerase (2.5 U/µL)	2 (5 U)
$MgSO_4$ 50 mM	1
Autoclaved milliQ water	To final volume 50 µL

Table 5. Standard PCR mix using high fidelity Invitrogen™ Pfx50™ DNA Polymerase.

It is noteworthy to say that every PCR has a negative control in which contains all the components excepting DNA template and it is run on agarose gel.

Step	Temperature (°C)	Time	
1	94	5 min	Initial template denaturation
2	94	30 s	Template denaturation
3	56	30 s	Annealing
4	68	1 min	Extension 1 min/kb DNA template
5	68	7 min	Final extension

Table 6. Thermocycling conditions for a PCR routine with Invitrogen™ Pfx50™ DNA Polymerase. Steps 2 to 4 are repeated 30 times.

3.2.5. Overlap extension PCR using Invitrogen™ Pfx50™ DNA Polymerase to fuse fragments AB, CD and EF

Overlap extension PCR (OE-PCR) is performed employing Invitrogen™ Pfx50™ DNA Polymerase essentially as described in Lee & al., 2004.

Component		Volume (µL)
10X Pfx50™ PCR Mix		10
10 mM dNTP Mix		2
Primers A and F		1.5 each primer (0.3 mM per primer)
DNA template*	Fragment AB	0.3 (10 ng)
	Fragment CD	0.2 (2 ng)
	Fragment EF	2 (20 ng)
Pfx50™ DNA Polymerase (2.5 U/µL)		2 (5 U)
$MgSO_4$ 50 mM		2
Autoclaved milliQ water		To final volume 50 µL

Table 7. Standard OE-PCR mix using Invitrogen™ Pfx50™ DNA Polymerase. *DNA template volume/amount is calculated to reach an equimolar ratio of three template fragments.

Step	Temperature (°C)	Time	
1	94	5 min	Initial template denaturation
2	94	30 s	Template denaturation
3	50	30 s	Annealing
4	68	1 min 45 s	Extension 1 min/kb DNA template
5	68	7 min	Final extension

Table 8. Thermocycling conditions for OE-PCR. Steps 2 to 4 are repeated 30 times.

3.2.6. DNA purification from agarose gels

Wizard® SV Gel and PCR Clean-Up System (Promega®) are employed in order to purify DNA fragments from agarose gels and remove excess of nucleotides and primers from PCR mixtures. This kit is based on the ability of DNA to bind to silica membranes in the presence of chaotropic salts which disrupt hydrogen bonding network. After electrophoresis to separate DNA fragments, the gel slice containing the DNA fragment of interest is excised, solved with Membrane Binding Solution that contains guanidine isothiocyanate, and purified with a microcolumn system and a Membrane Wash Solution diluted with 95% ethanol. DNA fragments are finally eluted from the microcolumn with 30 µL of Nuclease-Free Water, and the DNA concentration was determined with a NanoDrop spectrophotometer. A detailed protocol is found in the supplier website (Promega Corporation, 2010).

3.2.7. BP recombination reaction

Gateway™ BP Clonase™ II enzyme mix (Thermo Fisher Scientific®) was used to clone the *att*B-flanked DNA fragment, *TAT* ASAT in the *att*P-containing donor vector pDONR™ 207 to generate the corresponding *att*L-containing entry clone.

Component	**Volume (µL)**
*att*B-PCR product (*TAT* ASAT)	4 (50 ng)
Donor vector (pDONR™ 207)	1 (150 ng)
Gateway® BP Clonase® II enzyme mix	2
TE Buffer, pH 8.0	3

Table 9. BP reaction mix.

Components are added to a microcentrifuge tube at room temperature and after incubating the reaction at 25 °C for 1 hour, 1 µL of 2 µg/µL Proteinase K is added. The mixture is then incubated at 37 °C for 10 minutes to stop recombination reaction. This procedure is performed according to manufacturer's recommendations (Life Technologies Corporation, 2012).

3.2.8. LR recombination reaction

Recombination reaction between an *att*L-containing entry clone and an *att*R-containing destination vector pEarley Gate 103 to generate an expression clone.

Component	Volume (µL)
Entry clone (pDONR™ 207 + *TAT* ASAT)	4 (50 ng)
Destination vector (pEarley Gate 103)	1 (150 ng)
Gateway® LR Clonase® II enzyme mix	2
TE Buffer, pH 8.0	3

Table 10. LR recombination mix.

Components are added to a microcentrifuge tube at room temperature and after incubating the reaction at 25 °C for 1 hour, 1 µL of 2 µg/µL Proteinase K is added. The mixture is then incubated at 37 °C for 10 minutes to stop recombination reaction. This procedure is performed according to manufacturer's recommendations (Life Technologies Corporation, 2012).

3.2.9. Transformation of TOP10 *E. coli* competent cells

a) Aliquots (50 µL) of TOP10 competent cells are stored at -80 °C.
b) Take and leave cells on ice for 5 minutes.
c) Add 5 µL of the BP reaction, mix carefully and wait 2 minutes.
d) Incubate 30 seconds at 42 °C (heat shock)
e) Immediately place cells on ice for a minimum of 2 minutes.
f) Add 300 µL of liquid LB medium without antibiotics and incubate in a shaking incubator 1 h at 37 °C.
g) Spread 100 and 200 µL from each transformation on separate LB agar plates supplemented with 25 µg/mL of gentamicin (pDONR™ 207) or kanamycin (pEarley Gate 103).
h) Incubate at 37 °C overnight
i) Check the presence of recombinant plasmids in selected antibiotic resistant colonies by plasmid purification and PCR.

3.2.10. Plasmid DNA purification system from *E. coli* cell cultures

Wizard® Plus SV Minipreps DNA Purification System (Promega®) is employed so as to purify plasmid DNA from *E. coli* cell cultures. The quick protocol was performed according to manufacturer's recommendations (Promega Corporation, 2009).

3.2.11. Rapid method to distinguish mutant plants

CRISPR-Cas9 is a recombinant DNA technology used to generate permanent mutations by introducing double stranded breaks *in vitro* that activate the cell own DNA repair pathways giving rise to deletions or insertions, leading to mutant individuals, or resulting in full DNA repair, leading to wild-type individuals. This technology was used to generate tomato *psat* knock-out mutants (Figure 9).

The occurrence of mutations in the target gene is checked in all primary transformants (F_0 generation) by sequencing the region of interest, which has been previously amplified by PCR using genomic DNA as template and the PSAT gene specific primers shown in Figure 9, and cloned in the appropriate vector.

Afterwards, only plants showing a change in the open reading frame of the *PSAT* gene, so *psat* knock-out mutants, are selected for further characterization. In this case, the focus is on a heterozygous mutant plant called 31, which contains a 4 nucleotide deletion (Figure 10) that generates a new restriction site allowing the design of a restriction fragment length polymorphism (RFLP) method to facilitate the mutant selection process in the next generations.

>Solyc09g072710.2 | SL2.50ch09:65320648..65332727 reverse
TAAAAGTTTATCATTGAAAACTTTCCAATT***CCCAGCGGCAAAAAGTC***AGTCAGTTGTCC
CCAAAAGTTTACAATTTCCATGTGAAAAAACTGATAACAAATTGTTTCTAGCCAATGA
GAGGAGGACACGTGGGATTCGTCGTCATTTTCATTCTCCTAGCTACCGCCGGTAACCTT
GGCGGTGAGTTCGCCGGCGATTACTCGAAGCTΔGTCCGGAATTATTATCCCAGGATTCG
CGTCTACACAACTGAGAGCATGGTCAATATTAGACTGCCCTTATTCTCCTCTCGATTTC
AATCCTCT***CGATTTAGTCTGGCTCGACAC***TACTAAAGTAAATCTTCAACATTGGCTCTC

Fig. 9. The ATG translational start codon of the *PSAT* gene is shown in red. The position of the double stranded break generated by CRIPR/Cas9 is indicated by a red triangle and the nucleotide sequence preceding the break is framed in blue. The underlined nucleotide sequences shown in italics and bold correspond to the forward and reverse primers used to amplify the PSAT sequence encompassing the region where the double strand break is created.

Fig. 10. Alignment of the wild type and mutated PSAT sequence of heterozygous plant 31. The black arrowhead indicates the position of the break generated by the CRISPR-Cas9 system. The 4 nucleotide deletion in plant 31 is indicated by hyphens and the new *Xho*I restriction site is underlined in blue. The *Xho*I restriction site is also shown, with arrowheads indicating the cleavage site on each strand.

Component	**Volume (µL)**
*Xho*I Restriction Enzyme 10X Buffer	2
*Xho*I Restriction Enzyme (10 U/µL)	0.5 (5 U)
Acetylated BSA (10 µg/µL)	0.2
DNA (40 ng/µL)	12.5 (500 ng*)
Autoclaved milliQ water	To final volume 20 µL

Table 11. *Xho*I reaction mixture. After mixing the components in a sterile tube, incubate at 37 °C. *The supplier Promega® recommends 200-1500 ng of DNA for each 0.5 µL of enzyme.

After the digestion and subsequent analysis by agarose gel electrophoresis of the resulting fragments, a mutant individual with the 4 nucleotide deletion and the *Xho*I restriction site, will show two DNA fragments whereas a wild-type individual will show a single fragment due to the lack of this specific restriction site. Therefore, the result of a simple digestion with a restriction enzyme (RE) allows for rapid identification of these type of knock-out mutant plants.

Firstly, to test the reliability of the method, the RFLP assay was carried out using PSAT DNA sequences of wild type and mutant plant 31, whose genomic sequences encompassing the CRISPR-Cas9 target site had been already sequenced. Then, the RFLP method was used to determine whether plants 183-1 and 183-2, offsprings of F_0 plant 31, were *psat* homozygous or heterozygous mutants.

4. RESULTS AND DISCUSSION

4.1. DETECTION OF TOMATO *PSAT* KNOCK-OUT MUTANTS

In order to test the method designed to distinguish *psat* knock-out mutants created using the CRISPR-Cas 9 system, the RFLP assay, explained in section 3.2.11, was performed, firstly, using a 293-bp DNA fragment amplified by PCR from genomic DNA of *psat* heterozygous mutant plant 31 and wild-type plant 34.

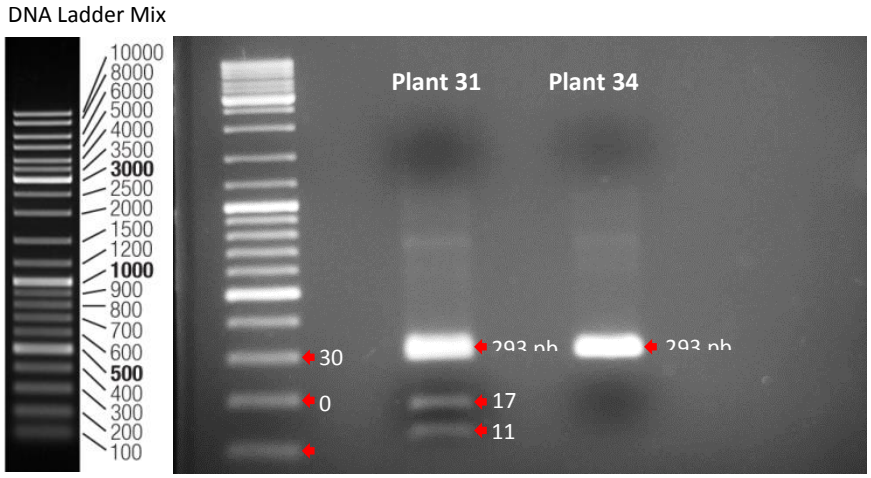

Fig. 11. Agarose gel (1.5%) electrophoresis of PSAT DNA fragments amplified by PCR from genomic DNA of heterozygous plant 31 and wild type plant 34 digested with *Xho*I.

As was expected, the digestion with *Xho*I of the PSAT DNA fragment from heterozygous plant 31 gives rise to three bands of 293, 174 and 118 bp, whereas that of DNA from plant 34 leads to a single band of 293 bp. These results are consistent with the heterozygosity of plant 31, since the uncut 293 bp fragment corresponds to the wild type allele while the 174 pb and 118 pb fragments are due to the presence of the *Xho*I site created by the CRISPR-Cas9 in the mutated allele. The single band in the sample from wild type plant 34 corresponds to the PSAT DNA entire fragment of 293 pb.

Once checked the reliability of the RFLP assay, *Xho*I digestion was employed to verify the mutant nature of plant 31 offsprings 183-1 and 183-2.

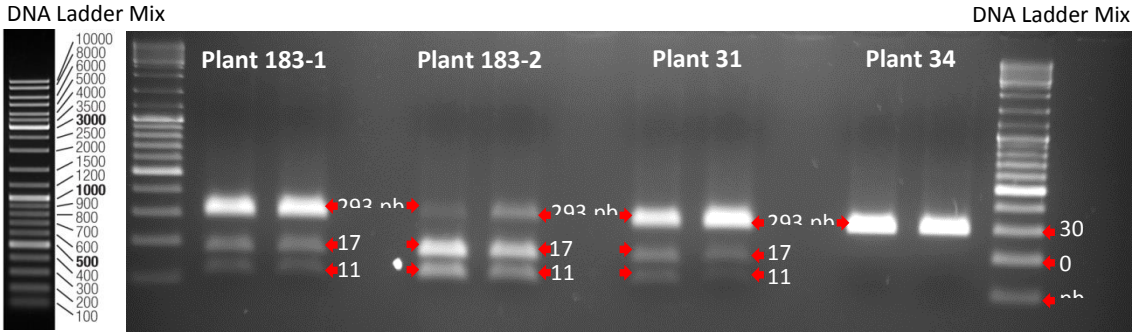

Fig. 12. Agarose (1.5%) gel electrophoresis of PSAT DNA fragments amplified by PCR from genomic DNA of plants 183-1, 183-2, 31 and 34 digested with *Xho*I.

As shown in Figure 12, three bands were obtained after the digestion with *Xho*I of PSAT DNA fragments amplified from genomic DNA of plants 183-1 and 183-2. These fragments have the same size than those obtained in the case of their predecessor, *psat* heterozygous plant 31: the upper band may have 293 pb, 174 pb the middle band and 118 the lower band. Therefore, these sequences contain an *Xho*I restriction site, which means that these plants are either heterozygous or homozygous *psat* mutants. It is noteworthy to pay attention to the relative intensity of the obtained bands. Concretely, the intensity of the upper band (293 bp) is higher than the other two bands (174 and 118 bp) in plant 183-1. This pattern of band intensity is identical to that observed in plant 31. On the contrary, in plant 183-2 the middle and lower bands show higher intensity than the upper band. These results indicated the heterozygosity of plant 183-1 and the homozygosity of plant 183-2, and demonstrated the validity of the RFLP test devised for a rapid and reliable screening of the progeny of this specific tomato *psat* mutant line.

4.2. OBTAINING A CHIMERIC *TAT* ASAT PROTEIN

Chimeric protein *TAT* ASAT, in which 101 central amino acids of SlASAT (positions 118 to 218, both included) were replaced by 18 amino acids of the equivalent region of AtASAT (positions 104 to 121, both included) was successfully obtained by OE-PCR.

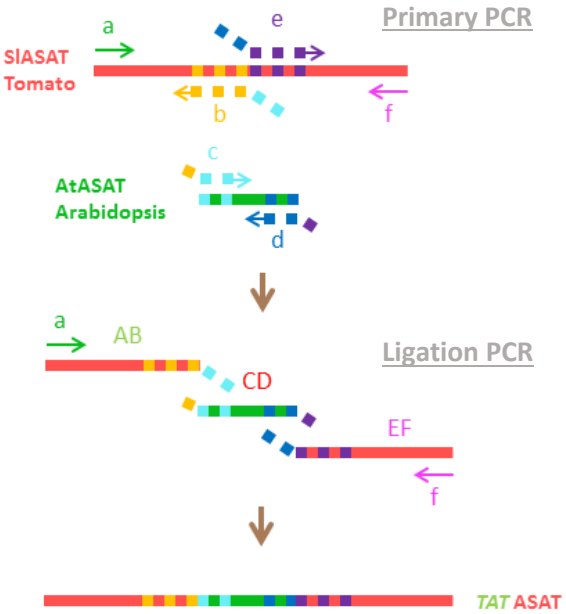

Fig. 13. Scheme of OE-PCR to obtain a chimeric cDNA coding for protein *TAT* ASAT. SlASAT and AtASAT sequences are denoted by red and green lines, respectively. Primers A and F are denoted by arrows and primers B to E are represented by squares in different colours. Squares of the same colour in primer and template sequences indicate sequence complementarity. The three PCR products (AB, CD and EF) obtained in separate PCR reactions (Primary PCR) with the appropriate primer pairs were mixed and amplified in a new PCR performed with the outermost primer pair A and F (Ligation PCR).

4.2.1. Primary PCR: obtaining of the three ASAT cDNA fragments

The three cDNA fragments, called AB, CD and EF, that once assembled would code for the *TAT* ASAT chimeric protein, were obtained by PCR, using as template pDONR™ 207 recombinant plasmids containing the SlASAT or AtASAT cDNA sequences, and primer pairs shown in Table 1. AB (391 pb) and EF (717 pb) fragments come from SlASAT, and CD (73 pb) from AtASAT. Firstly, a gradient PCR (temperature range 50.7-67.4°C) was performed using Green *Taq* DNA Polymerase, as describe in section 3.2.3, to experimentally determine the best annealing temperature for each pair of primers.

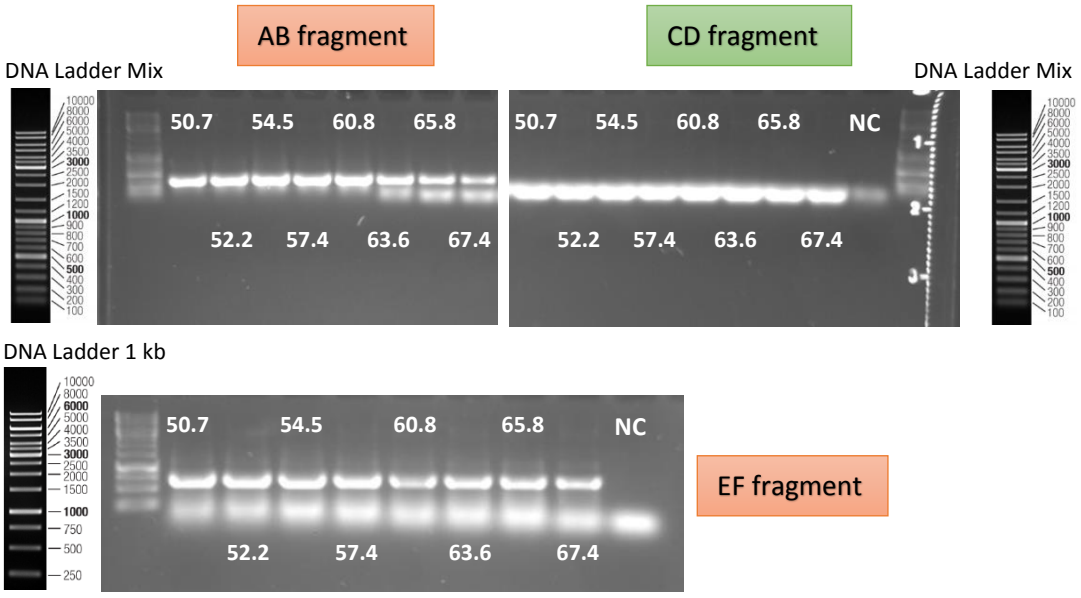

Fig. 14. Agarose (1% gel) gel showing the PCR products obtained at the indicated annealing temperatures. NC means negative control lacking template DNA.

As shown in Figure 14, major bands corresponding to PCR products of the expected size were obtained in all three cases. According to the intensity of the bands and the lack of additional DNA fragments, 56°C was selected as the optimum annealing temperature. Thus, the next PCRs to obtain fragments AB, CD and EF by the high-fidelity Pfx50™ DNA Polymerase, were done in duplicate at 56 °C in the annealing step, as described in section 3.2.4. The resulting PCR products were fractionated by agarose gel electrophoresis (Fig. 15) and purified, as defined in section 3.2.6.

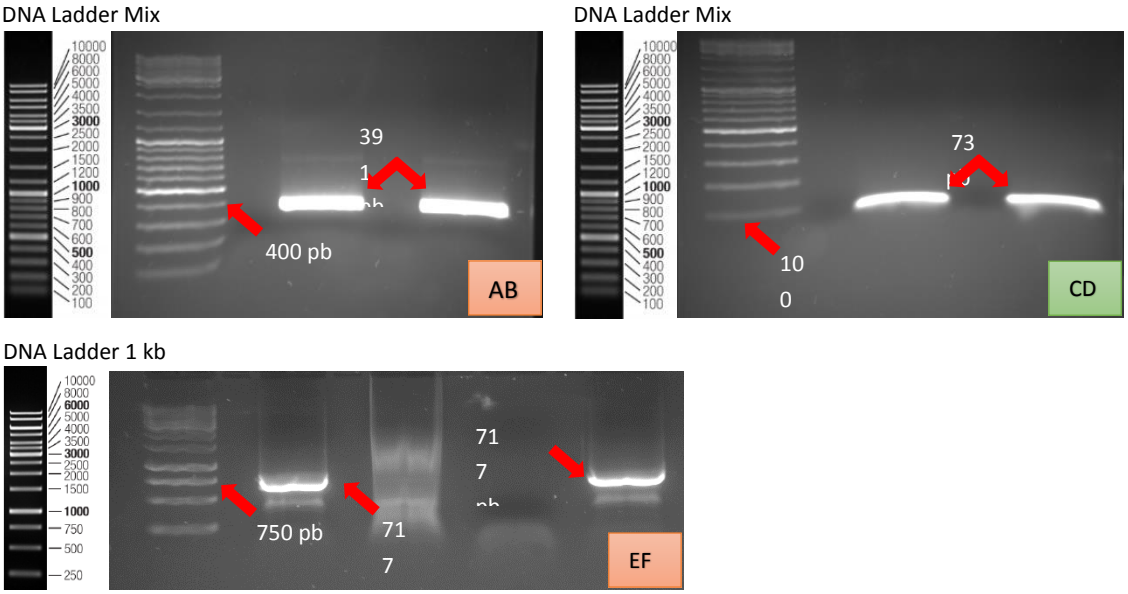

Fig. 15. Preparative agarose (1.2%) gel electrophoresis showing the amplified AB, CD and EF cDNA fragments.

Fragment	Concentration (ng/ µL)	Fragment	Concentration (ng/µL)
AB.1	32.84	CD.2	9.75
AB.2	33.91	EF.1	98.62
CD.1	10.18	EF.2	97.35

Table 12. Concentration of each purified fragment of DNA was determined with a NanoDrop spectrophotometer. Fragments on the right side of the images in Figure 15 are considered as 1, and those on the left side are referred to as 2.

4.2.2. Ligation PCR: obtaining a cDNA encoding *TAT* ASAT

The three overlapping fragments AB, CD and EF were fused to obtain the complete sequence of a cDNA coding for *TAT* ASAT, by ligation PCR with Pfx50™ DNA Polymerase and primers a and f, as described in section 3.2.5. The temperature of annealing selected was 50 °C according to the T_m of primers a and f, and the protruding complementary

ends of fragments that hybridize as primers. Two different PCR reactions with 50 and 100 ng of template DNA (considering the three fragments together) were carried out, and the results are shown in Figure 16. In both cases a DNA fragment of the expected size (1184 bp) was obtained, thus suggesting that the cDNA *TAT* ASAT was successfully created. The DNA fragments were purified from the gel, as defined in section 3.2.6, and the concentration of the purified fragments was determined. The concentrations of DNA obtained were 21.0, 14.6, 103.7 and 96.9 ng/µL (left to right in Figure 16), respectively.

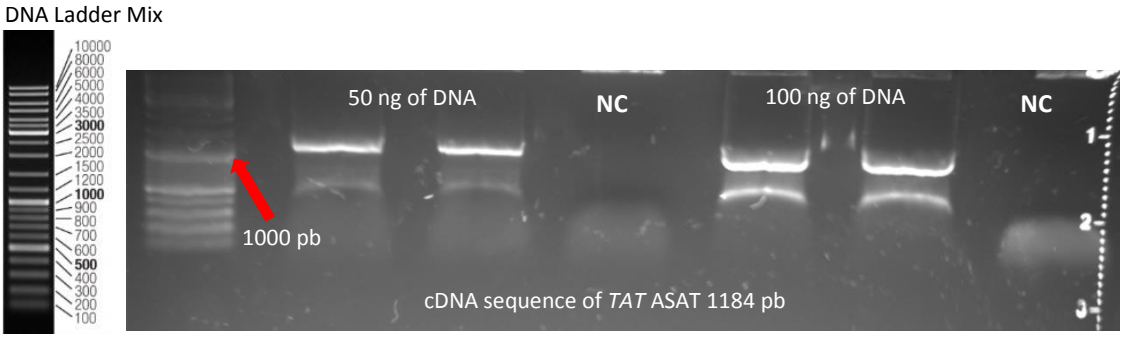

Fig. 16. Agarose (1.2%) gel electrophoresis showing the results of overlapping PCR to generate a cDNA sequence coding for *TAT* ASAT. The first 2 lanes on the left side show the result of a PCR performed with 50 ng of DNA template, whereas those on the right side correspond to a PCR performed with 100 ng of template. According to GeneRuler DNA Ladder Mix, the length of the entire fragment was compatible with its expected size (1184 pb). NC means Negative Control lacking template DNA.

4.2.4 Cloning the cDNA *TAT* ASAT into a Gateway® vector

Through BP reaction, as described in section 3.2.7, the *TAT* ASAT cDNA sequence was inserted into pDONR™ 207 vector establishing an entry clone. Afterwards, TOP10 *E. coli* cells were transformed, as defined in section 3.2.9, and grown on LB agar medium plates supplemented with gentamycin. Plasmid DNA from 10 gentamycin resistant colonies was purified and the presence of the insert was assessed by PCR (Fig. 17) using Green *Taq* DNA polymerase and 50 °C of annealing temperature, as determined in section 3.2.3, and primers a and f, shown in table 1.

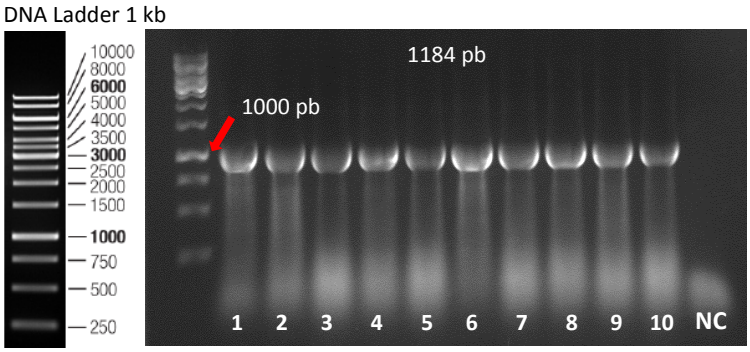

Fig. 17. Agarose (1%) gel electrophoresis showing the results of cDNA *TAT* ASAT amplification by PCR using plasmid DNA from transformed TOP10 *E. coli* colonies (1-10) as template. NC means Negative Control lacking template DNA.

All colonies were found to contain the chimeric cDNA and the insert of a selected plasmid was sequenced at the sequencing service of the CRAG. The sequence of the cloned fragment was identical to the expected one, thus confirming that the chimeric *TAT* ASAT cDNA was successfully created. The cDNA was then transferred to pEarley Gate 103 vector by recombination reaction LR, as defined in section 3.2.8. After transforming TOP10 *E. coli* cells using the method described in section 3.2.9, bacterial cells were grown on LB agar medium plates supplemented with kanamycin. The presence of the cDNA fragment in plasmids purified from resistant colonies was tested by PCR employing Green *Taq* DNA polymerase at 54 °C of annealing temperature, as determined in section 3.2.3, with primers e and GFP. Primer GFP vas used because in this vector the cloned insert is fused to the 5'-end of the sequence encoding GFP, which enables subsequent expression of the protein of interest fused C-terminal to the GFP. The expected length of the PCR product was 920 pb.

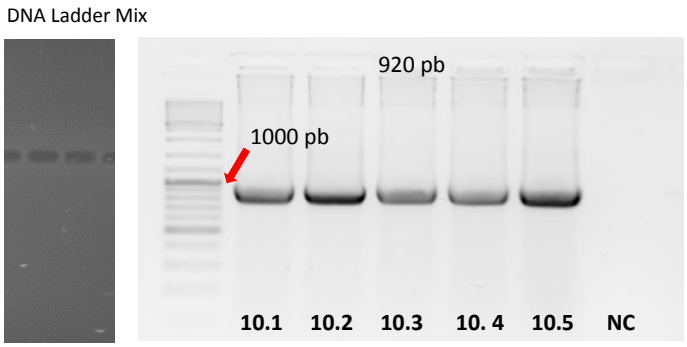

Fig. 18 Agarose (1%) gel electrophoresis showing the results of *TAT* ASAT cDNA fused to GFP coding sequence amplification by PCR using as template plasmid DNA from 5 TOP10 *E. coli* colonies. NC means Negative Control lacking template DNA.

The DNA region encompassing the fusion between the sequences encoding *TAT* ASAT and the GFP was sequenced to ensure that both coding sequences were in-frame.

At that point, the cDNA sequence coding for the *TAT* ASAT-GFP chimeric protein was successfully obtained and inserted into the binary pEarley Gate 103 expression vector, ready to proceed to transformation into *Agrobacterium tumefaciens* cells for subsequent agroinfiltration of *Nicotiana benthamiana* leaves to carry out subcellular localization studies using confocal microscopy techniques. The predicted membrane topology model of *TAT* ASAT chimeric protein performed with the Protter 1.0 program (Omasits & al., 2014) is shown in Figure 19.

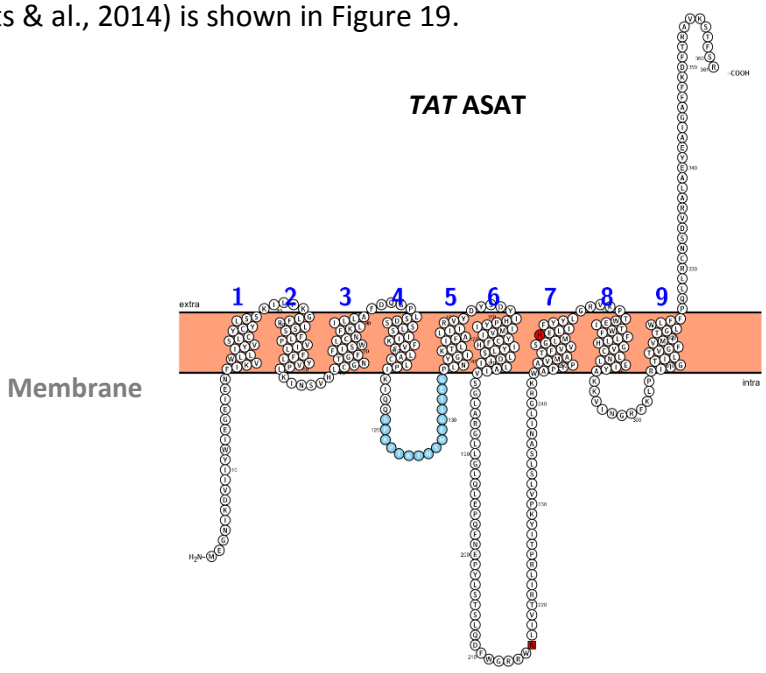

Fig. 19. Membrane topology model of *TAT* ASAT chimeric protein. The transmembrane sequences are numbered in blue. The Asn and His residues reportedly important for ASAT catalysis are shown in red. The sequence of 18 amino acids comprised between positions 104 to 121, both included, in the AtASAT1 sequence that replaces the 101 amino acid residues comprised between positions 118 to 218, both included, in the SlASAT1 sequence, is shown in blue.

5. CONCLUSIONS

Regarding the first objective, a Restriction Fragment Length Polimorfism (RFLP) strategy based on digestion of a PCR-amplified *PSAT* genomic fragment with *Xho*I restriction enzyme has been implemented as a rapid and efficient method to discriminate whether tomato *psat* knock-out mutants generated by CRISPR-Cas9 are homozygous or herozygous for the mutant allele, and distinguish them from wild-type individuals.

Concerning the second objective, a hybrid *TAT* ASAT cDNA sequence which encodes a chimeric ASAT protein of 361 amino acids consisting of the first N-terminal 117 amino acids of SlASAT, followed by 18 amino acids corresponding to the central domain of AtASAT, and the C-terminal 226 amino acids of SlASAT, has been created by overlap extension PCR.

The *TAT* ASAT coding sequence has been cloned in-frame with the GFP coding sequence into the binary pEarley Gate 103 vector, so that the chimeric *TAT* ASAT protein can be constitutively expressed in plants joined to the N-terminal end of GFP. The fluorescence provided by GFP will allow future subcellular location studies to be addressed in order to determine whether the central protein domain is involved or not in the differential subcellular location of SlASAT and AtASAT or if it may affect enzyme activity.

BIBLIOGRAPHY

Banaś, A., Carlsson, A. S., Huang, B., Lenman, M., Banaś, W., Lee, M., Noiriel, A., Benveniste, P., Schaller, H., Bouvier-Navé, P., & Stymne, S. 2005. Cellular sterol ester synthesis in plants is performed by an enzyme (phospholipid:Sterol acyltransferase) different from the yeast and mammalian acyl-CoA:Sterol acyltransferases. *J. Biol. Chem.*, 280: 34626–34634. https://doi.org/10.1074/jbc.M504459200

Bouvier-Nave, P., Berna, A., Noiriel, A., Compagnon, V., Carlsson, A. S., Banas, A., Stymne, S., & Schaller, H. 2010. Involvement of the Phospholipid Sterol Acyltransferase1 in Plant Sterol Homeostasis and Leaf Senescence. *Plant Physiol.*, 152: 107–119. https://doi.org/10.1104/pp.109.145672

Chen, Q., Steinhauer, L., Hammerlindl, J., Keller, W., & Zou, J. 2007. Biosynthesis of Phytosterol Esters: Identification of a Sterol O-Acyltransferase in Arabidopsis. *Plant Physiol.*, 145: 974–984. https://doi.org/10.1104/pp.107.106278

Duperon, R., Thiersault, M., & Duperon, P. 1984. High level of glycosylated sterols in species of solanum and sterol changes during the development of the tomato. *Phytochemistry*, 23: 743–746. https://doi.org/10.1016/S0031-9422(00)85016-5

Dyas, L., & Goad, L. J. 1993. Steryl fatty acyl esters in plants. *Phytochemistry*, 34: 17–29. https://doi.org/10.1016/S0031-9422(00)90777-5

European Bioinformatics Institute (EMBL-EBI). 2016. Clustal Omega. Program distributed by the author. Wellcome Genome Campus, Hinxton, Cambridgeshire. https://www.ebi.ac.uk/Tools/msa/clustalo/

Ferrer, A., Altabella, T., Arró, M., & Boronat, A. 2017. Emerging roles for conjugated sterols in plants. *Prog. Lipid Res.*, 67: 27–37. https://doi.org/10.1016/j.plipres.2017.06.002

Giovannoni, J. 2004. Genetic regulation of fruit development and ripening. *Plant Cell Online*, 16: 170–181. https://doi.org/10.1105/tpc.019158.Fruit

GSL Biotech. 2018. SnapGene software. Program distributed by the author. Chicago, IL. http://www.snapgene.com/

Harker, M., Hellyer, A., Clayton, J. C., Duvoix, A., Lanot, A., & Safford, R. 2003. Co-ordinate regulation of sterol biosynthesis enzyme activity during accumulation of sterols in developing rape and tobacco seed. *Planta*, 216: 707–715. https://doi.org/10.1007/s00425-002-0913-3

Hartmann, M. A. 1998. Plant sterols and the membrane environment. *Trends Plant Sci.*, 3: 170–175. https://doi.org/10.1016/S1360-1385(98)01233-3

Kopischke, M., Westphal, L., Schneeberger, K., Clark, R., Ossowski, S., Wewer, V., Fuchs, R., Landtag, J., Hause, G., Dörmann, P., Lipka, V., Weigel, D., Schulze-Lefert, P., Scheel, D., & Rosahl, S. 2013. Impaired sterol ester synthesis alters the response of Arabidopsis thaliana to Phytophthora infestans. *Plant J.*, 73: 456–468. https://doi.org/10.1111/tpj.12046

Lee, J., Lee, H. J., Shin, M. K., & Ryu, W. S. 2004. Versatile PCR-mediated insertion or deletion mutagenesis. *Biotechniques*, 36: 398–400.

Life Technologies Corporation. 2012. Gateway ® Technology with Clonase ™ II A universal technology to clone DNA. https://tools.thermofisher.com/content/sfs/manuals/gateway_clonaseii_man.pdf (accessed 22 Feb 2018).

Moreau, R. A., Whitaker, B. D., & Hicks, K. B. 2002. Phytosterols, phytostanols, and their conjugates in foods: Structural diversity, quantitative analysis, and health-promoting uses. *Prog. Lipid Res.*, 41: 457–500. https://doi.org/10.1016/S0163-7827(02)00006-1

Murphy, D. J. 2012. The dynamic roles of intracellular lipid droplets: From archaea to mammals. *Protoplasma*, 249: 541–585. https://doi.org/10.1007/s00709-011-0329-7

Netala, V. R., Ghosh, S. B., Bobbu, P., Anitha, D., & Tartte, V. 2015. Triterpenoid saponins: A review on biosynthesis, Applications and mechanism of their action. *Int. J. Pharm. Pharm. Sci.*, 7: 24–28.

Nyström, L., Schär, A., & Lampi, A. M. 2012. Steryl glycosides and acylated steryl glycosides in plant foods reflect unique sterol patterns. *Eur. J. Lipid Sci. Technol.*, 114: 656–669. https://doi.org/10.1002/ejlt.201200033

Omasits, U., Ahrens, C. H., Müller, S., & Wollscheid, B. 2014. Protter: Interactive protein feature visualization and integration with experimental proteomic data. *Bioinformatics*, 30: 884–886. https://doi.org/10.1093/bioinformatics/btt607

Ostlund, R. E. 2002. Phytosterols in human nutrition. *Annu. Rev. Nutr.*, 22: 533–549. https://doi.org/10.1146/annurev.nutr.22.020702.075220

Promega Corporation. 2009. Wizard Plus SV Minipreps DNA Purification System Protocol. https://www.promega.es/-/media/files/resources/protcards/wizard-plus-sv-minipreps-dna-purification-system-quick-protocol.pdf?la=es-es. (accessed 22 Feb 2018).

Promega Corporation. 2010. Wizard ® SV Gel and PCR Clean-Up System Wizard ® SV Gel and PCR Clean-Up System. https://tools.thermofisher.com/content/sfs/manuals/gateway_clonaseii_man.pdf (accessed 22 Feb 2018).

Ramirez-Estrada, K., Castillo, N., Lara, J. A., Arró, M., Boronat, A., Ferrer, A., & Altabella, T. 2017. Tomato UDP-Glucose Sterol Glycosyltransferases: A Family of Developmental and Stress Regulated Genes that Encode Cytosolic and Membrane-Associated Forms of the Enzyme. *Front. Plant Sci.*, 8: 984. https://doi.org/10.3389/fpls.2017.00984

Schaller, H. 2004. New aspects of sterol biosynthesis in growth and development of higher plants. *Plant Physiol. Biochem.*, 42: 465–476. https://doi.org/10.1016/j.plaphy.2004.05.012

Vranová, E., Coman, D., & Gruissem, W. 2012. Structure and dynamics of the isoprenoid pathway network. *Mol. Plant*, 5: 318–333. https://doi.org/10.1093/mp/sss015

Wang, H., Nagegowda, D. A., Rawat, R., Bouvier-Navé, P., Guo, D., Bach, T. J., & Chye, M. L. 2012. Overexpression of Brassica juncea wild-type and mutant HMG-CoA synthase 1 in Arabidopsis up-regulates genes in sterol biosynthesis and enhances sterol production and stress tolerance. *Plant Biotechnol. J.*, 10: 31–42. https://doi.org/10.1111/j.1467-7652.2011.00631.x

Whitaker, B. D. 1988. Changes in the steryl lipid content and composition of tomato fruit during ripening. *Phytochemistry*, 27: 3411–3416.

ANNEXES

1. Tomato ASAT1 (SlASAT) protein and cDNA sequences

```
atggagggaaatattaaagatgttatcatatattggatagaaggagaaattgaaaatttt
 M  E  G  N  I  K  D  V  I  I  Y  W  I  E  G  E  I  E  N  F
attaaggtatggttattaatttatgtatcactttgttattgttatttatcatctaaaatt
 I  K  V  W  L  L  I  Y  V  S  L  C  Y  C  Y  L  S  S  K  I
cttccaaaaggtttatttaggctctcttctttttaccagtgatattatttttcctttat
 L  P  K  G  L  F  R  L  S  S  F  L  P  V  I  L  F  F  L  Y
gttccacttaaaattaattctgttcatctttgtggtaatactggtttttttcatttcttgg
 V  P  L  K  I  N  S  V  H  L  C  G  N  T  G  F  F  I  S  W
ctttgtaattttaaacttattttacttgcttttgaccaaggtccactttctgattcttca
 L  C  N  F  K  L  I  L  L  A  F  D  Q  G  P  L  S  D  S  S
ctttctattattaaatttgtttttcttgcttgtttacctatcaagattcaacaaaaatct
 L  S  I  I  K  F  V  F  L  A  C  L  P  I  K  I  Q  Q  K  S
caaatttatgtggaaaatagagataaatttcatcaaaataatcattttcaagaaacccca
 Q  I  Y  V  E  N  R  D  K  F  H  Q  N  N  H  F  Q  E  T  P
tctaatgaaaaaaaggattttgcaaaaaatgaccattttcaagaaactcaatttccaagc
 S  N  E  K  K  D  F  A  K  N  D  H  F  Q  E  T  Q  F  P  S
tcaattgataaaattgaaaacaacccttttcaagatggttatttttatgaaaccccatct
 S  I  D  K  I  E  N  N  P  F  Q  D  G  Y  F  Y  E  T  P  S
aagaagttagttgaaaatggttctagtgtgcaaaatggaaaggattttgcaaaaagtggc
 K  K  L  V  E  N  G  S  S  V  Q  N  G  K  D  F  A  K  S  G
tattttaaagaaagttcagttccctcttttgcaaagtccaacaaaggtcaaaagttaaat
 Y  F  K  E  S  S  V  P  S  F  A  K  S  N  K  G  Q  K  L  N
tatggcataaagacacttatttttgctttaattattagagtttatgactatagtgattat
 Y  G  I  K  T  L  I  F  A  L  I  I  R  V  Y  D  Y  S  D  Y
atacatccctatataattatggtcatatattgcttccacatttaccttagcttagatatt
 I  H  P  Y  I  I  M  V  I  Y  C  F  H  I  Y  L  S  L  D  I
attctagctattgtttcgggcttggcccgcgggcttctcgggcttcagctagagccacag
 I  L  A  I  V  S  G  L  A  R  G  L  L  G  L  Q  L  E  P  Q
ttcaatgaaccgtatttatcaacttcactacaagatttttggggccggcgttggaatctc
 F  N  E  P  Y  L  S  T  S  L  Q  D  F  W  G  R  R  W  N  L
attgtcactcgtatccttaggcccactatatataagcccgttctaagcctctccgcgaat
 I  V  T  R  I  L  R  P  T  I  Y  K  P  V  L  S  L  S  A  N
attttgggccgaaagtgggccccaattcccgcggtgatggctacatttgttgtttcgggc
 I  L  G  R  K  W  A  P  I  P  A  V  M  A  T  F  V  V  S  G
cttatgcatgagctgatattttactatttgggccgggttaagcccacttgggagatcact
 L  M  H  E  L  I  F  Y  Y  L  G  R  V  K  P  T  W  E  I  T
tggttctttttgctacatggggtttgtttgaacctagagatttatgctaagaaggtgatc
 W  F  F  L  L  H  G  V  C  L  N  L  E  I  Y  A  K  K  V  I
aacggtagatttaagctcccacggataatcgggacaatcttgaccgttggattcgttatg
 N  G  R  F  K  L  P  R  I  I  G  T  I  L  T  V  G  F  V  M
atcacgggtttgtggctatttttttcctcaattgttacggtgtaattctgatgttagagct
 I  T  G  L  W  L  F  F  P  Q  L  L  R  C  N  S  D  V  R  A
cttgcagagtatgaagcaattggtgcattctttaaggatttcactagggctgtgaaatca
 L  A  E  Y  E  A  I  G  A  F  F  K  D  F  T  R  A  V  K  S
acattttcgagataa
 T  F  S  R  -
```

Fragment AB

Fragment EF

Fragments AB and EF from SlASAT cDNA define the 5' and 3' outermost regions of *TAT* ASAT cDNA sequence, respectively. AB has 351 pb and encodes a sequence of 117 amino acids. The length of the amplified fragment is 391 pb since it includes the primer tails

(section 4.2.2). Likewise, fragment EF has 678 pb, 717 pb including primer tails, and encodes a sequence of 226 amino acids.

Primers A and F hybridize to the 5' and 3' ends of fragments AB and EF, respectively, and are shown in blue and italics. Sequences where primers B and E hybridize are shown underlined and in colour blue and violet, and only the nucleotides shown in violet correspond to primers C and D.

2. Arabidopsis ASAT (AtASAT) protein and cDNA sequences

```
atggcgagtttcatcaaggcatggggtttagtgatcatctcactgtgttacacttttttc
 M  A  S  F  I  K  A  W  G  L  V  I  I  S  L  C  Y  T  F  F
attgccaaattggttccaaaaggaatcaaaaggctcatactatttttccctgtcttcctc
 I  A  K  L  V  P  K  G  I  K  R  L  I  L  F  F  P  V  F  L
attttcttcatagtacctttcttgatatattccttacatttactcggcatcacggctttc
 I  F  F  I  V  P  F  L  I  Y  S  L  H  L  L  G  I  T  A  F
ttcatcgcttggctagcaaatttcaagctcttattatttgcattagggcgcggtcctctc
 F  I  A  W  L  A  N  F  K  L  L  L  F  A  L  G  R  G  P  L
tcttcaaaccataaacccctatctctccctatttttcttagctgtctcttgcttgcccatc
 S  S  N  H  K  P  L  S  L  P  I  F  L  A  V  S  C  L  P  I
aagattcagctgagcccaaaacctacaaaaactcactcccatgaaggatccacagagggt
 K  I  Q  L  S  P  K  P  T  K  T  H  S  H  E  G  S  T  E  G
ccttgatttataccataaaggcagtttttgtggttctcatcatcaaagcctacgaatac
 P  L  I  Y  T  I  K  A  V  F  V  V  L  I  I  K  A  Y  E  Y
agtaccaaattgcctgagaaagtcgtgctgactctctacgcgatccacatatatttcgcc
 S  T  K  L  P  E  K  V  V  L  T  L  Y  A  I  H  I  Y  F  A
cttgagatcatccttgccgccacagctgctgcggttcgagccatgtcggatcttgagctc
 L  E  I  I  L  A  A  T  A  A  A  V  R  A  M  S  D  L  E  L
gagccacagttcaacaagccgtacctagcgacatcacttcaagatttctgggggagacga
 E  P  Q  F  N  K  P  Y  L  A  T  S  L  Q  D  F  W  G  R  R
tggaacctgatggtcactggaatcttacggccaaccgtgtacgaaccgtcacttcaactg
 W  N  L  M  V  T  G  I  L  R  P  T  V  Y  E  P  S  L  Q  L
ttctcggttttgggcccgaactattcccagattcttgcagctttcgggacgtttgttgtc
 F  S  V  L  G  P  N  Y  S  Q  I  L  A  A  F  G  T  F  V  V
tctgggataatgcacgagctcatcttcttctacatgggacggttgaggccagactggaag
 S  G  I  M  H  E  L  I  F  F  Y  M  G  R  L  R  P  D  W  K
atgatgtggttcttcctcataaatggattttgcacgaccgtggagatcgccatcaagaaa
 M  M  W  F  F  L  I  N  G  F  C  T  T  V  E  I  A  I  K  K
accattaacggtaggtggagattcccgaaagcaatcagtcaggttttgacactcacttttt
 T  I  N  G  R  W  R  F  P  K  A  I  S  Q  V  L  T  L  T  F
gtgatggtgacggcattgtggctgttcttgcccgaatttaatcggtgcaacatagttgag
 V  M  V  T  A  L  W  L  F  L  P  E  F  N  R  C  N  I  V  E
aaggctcttgatgagtacgcagccataggcgcatttgcagtcgaggtcaggaggaaactg
 K  A  L  D  E  Y  A  A  I  G  A  F  A  V  E  V  R  R  K  L
accgcatatctttttaa
 T  A  Y  L  F  -
```

Fragment CD

Fragment CD (underlined) from AtASAT cDNA defines the central region of *TAT* ASAT cDNA sequence. CD has 54 pb and encodes a sequence of 18 amino acids. In section 4.2.2, the length of the amplified fragment is 73 pb, including the primer tails.

Primers C and D hybridize to sequences shown underlined and in colour blue and violet. Sequences where primers B and E hybridize are shown underlined and in colour violet.

3. *TAT* ASAT cDNA open reading frame

```
atggagggaaatattaaagatgttatcatatattggatagaaggagaaattgaaaatttt
 M  E  G  N  I  K  D  V  I  I  Y  W  I  E  G  E  I  E  N  F
attaaggtatggttattaatttatgtatcactttgttattgttatttatcatctaaaatt
 I  K  V  W  L  L  I  Y  V  S  L  C  Y  C  Y  L  S  S  K  I
cttccaaaaggtttatttaggctctcttctttttttaccagtgatattatttttcctttat
 L  P  K  G  L  F  R  L  S  S  F  L  P  V  I  L  F  F  L  Y
gttccacttaaaattaattctgttcatctttgtggtaatactggtttttttcatttcttgg
 V  P  L  K  I  N  S  V  H  L  C  G  N  T  G  F  F  I  S  W
ctttgtaattttaaacttattttacttgcttttgaccaaggtccactttctgattcttca
 L  C  N  F  K  L  I  L  L  A  F  D  Q  G  P  L  S  D  S  S
ctttctattattaaatttgtttttcttgcttgtttacctatcaagattcaactgagccca
 L  S  I  I  K  F  V  F  L  A  C  L  P  I  K  I  Q  L  S  P
aaacctacaaaaactcactcccatgaaggatccacagagggtctttaaattatggcata
K  P  T  K  T  H  S  H  E  G  S  T  E  G  P  L  N  Y  G  I
aagacacttatttttgctttaattattagagtttatgactatagtgattatatacatccc
 K  T  L  I  F  A  L  I  I  R  V  Y  D  Y  S  D  Y  I  H  P
tatataattatggtcatatattgcttccacatttaccttagcttagatattattctagct
 Y  I  I  M  V  I  Y  C  F  H  I  Y  L  S  L  D  I  I  L  A
attgtttcgggcttggcccgcgggcttctcgggcttcagctagagccacagttcaatgaa
 I  V  S  G  L  A  R  G  L  L  G  L  Q  L  E  P  Q  F  N  E
ccgtatttatcaacttcactacaagatttttggggccggcgttggaatctcattgtcact
 P  Y  L  S  T  S  L  Q  D  F  W  G  R  R  W  N  L  I  V  T
cgtatccttaggcccactatatataagcccgttctaagcctctccgcgaatattttgggc
 R  I  L  R  P  T  I  Y  K  P  V  L  S  L  S  A  N  I  L  G
cgaaagtgggccccaattcccgcggtgatggctacatttgttgtttcgggccttatgcat
 R  K  W  A  P  I  P  A  V  M  A  T  F  V  V  S  G  L  M  H
gagctgatattttactatttgggccgggttaagcccacttgggagatcacttggttcttt
 E  L  I  F  Y  Y  L  G  R  V  K  P  T  W  E  I  T  W  F  F
ttgctacatggggtttgtttgaacctagagatttatgctaagaaggtgatcaacggtaga
 L  L  H  G  V  C  L  N  L  E  I  Y  A  K  K  V  I  N  G  R
tttaagctcccacggataatcgggacaatcttgaccgttggattcgttatgatcacgggt
 F  K  L  P  R  I  I  G  T  I  L  T  V  G  F  V  M  I  T  G
ttgtggctatttttttcctcaattgttacggtgtaattctgatgttagagctcttgcagag
 L  W  L  F  F  P  Q  L  L  R  C  N  S  D  V  R  A  L  A  E
tatgaagcaattggtgcattctttaaggatttcactagggctgtgaaatcaacattttcg
 Y  E  A  I  G  A  F  F  K  D  F  T  R  A  V  K  S  T  F  S
aga
 R
```

Fusion of fragments AB (red), CD (green) and EF (red) to generate *TAT* ASAT cDNA sequence. Start codon (ATG) is shown in blue. The final length of the open reading frame (ORF) is 1086 pb. There is no stop codon at the 3'-end of the ORF because it had to be fused in-frame with the coding region of GFP.